






ORIGINAL RESEARCH

Open Access



Biochar reduced the mineralization of native and added soil organic carbon: evidence of negative priming and enhanced microbial carbon use efficiency

Subin Kalu^{1,2,3*} , Aino Seppänen¹, Kevin Z. Mganga^{1,4} , Outi-Maaria Sietiö^{1,5} , Bruno Glaser⁶  and Kristiina Karhu^{1,7} 

Abstract

Biochar has been widely recognized for its potential to increase carbon (C) sequestration and mitigate climate change. This potential is affected by how biochar interacts with native soil organic carbon (SOC) and fresh organic substrates added to soil. However, only a few studies have been conducted to understand this interaction. To fill this knowledge gap, we conducted a ¹³C-glucose labelling soil incubation for 6 months using fine-textured agricultural soil (Stagnosol) with two different biochar amounts. Biochar addition reduced the mineralization of SOC and ¹³C-glucose and increased soil microbial biomass carbon (MBC) and microbial carbon use efficiency (CUE). The effects were found to be additive i.e., higher biochar application rate resulted in lower mineralization of SOC and ¹³C-glucose. Additionally, soil density fractionation after 6 months revealed that most of the added biochar particles were recovered in free particulate organic matter (POM) fraction. Biochar also increased the retention of ¹³C in free POM fraction, indicating that added ¹³C-glucose was preserved within the biochar particles. The measurement of ¹³C from the total amino sugar fraction extracted from the biochar particles suggested that biochar increased the microbial uptake of added ¹³C-glucose and after they died, the dead microbial residues (necromass) accumulated inside biochar pores. Biochar also increased the proportion of occluded POM, demonstrating that increased soil occlusion following biochar addition reduced SOC mineralization. Overall, the study demonstrates the additional C sequestering potential of biochar by inducing negative priming of native SOC as well as increasing CUE, resulting in the formation and stabilization of microbial necromass.

Highlights

- Biochar showed additional C storage ability by preserving SOC from mineralization (negative priming) and stabilizing added labile organic substrate
- Biochar (30 Mg ha⁻¹) significantly increased microbial carbon use efficiency
- Biochar increased the formation of stable microbial residues (necromass) from a labile substrate (glucose) added to soil, as indicated by ¹³C recovery in amino sugars

Handling editor: Xiaoyuan Yan

*Correspondence:

Subin Kalu

subin.kalu@helsinki.fi

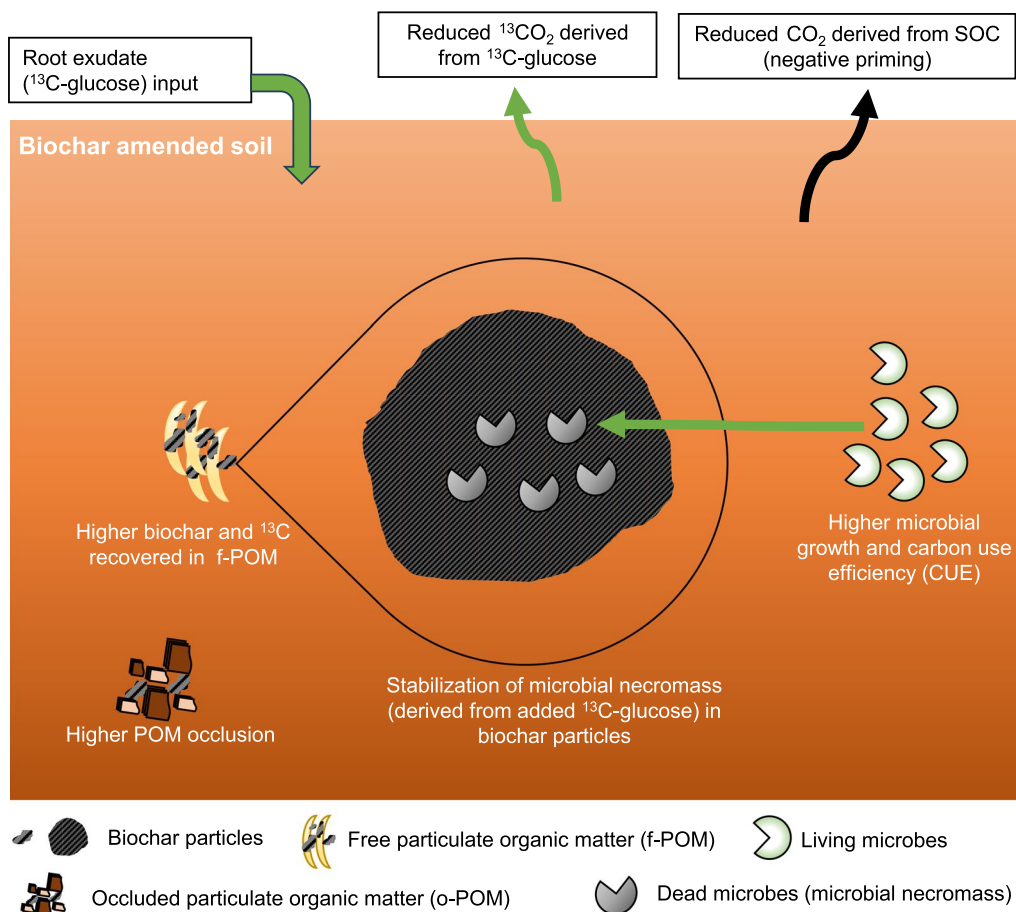
Full list of author information is available at the end of the article



© The Author(s) 2024. **Open Access** This article is licensed under a Creative Commons Attribution 4.0 International License, which permits use, sharing, adaptation, distribution and reproduction in any medium or format, as long as you give appropriate credit to the original author(s) and the source, provide a link to the Creative Commons licence, and indicate if changes were made. The images or other third party material in this article are included in the article's Creative Commons licence, unless indicated otherwise in a credit line to the material. If material is not included in the article's Creative Commons licence and your intended use is not permitted by statutory regulation or exceeds the permitted use, you will need to obtain permission directly from the copyright holder. To view a copy of this licence, visit <http://creativecommons.org/licenses/by/4.0/>.

Keywords Biochar, Carbon sequestration, Carbon use efficiency, ¹³C-labelling, Soil microbial necromass, Priming effect

Graphical Abstract



1 Introduction

The sequestration of atmospheric CO₂ into soil organic carbon (SOC) has been identified as a major strategy to combat climate change (Field and Mach 2017; Minasny et al. 2017; IPCC 2022). Therefore, it is imperative to identify soil management practices that not only increase soil C storage (and its associated benefits to agriculture) but also counteract the depletion of SOC (Kopittke et al. 2022). Biochar amendment to agricultural soils has been well-recognized for its potential in soil C sequestration and mitigating climate change (Woolf et al. 2010; Gross et al. 2021; Lehmann et al. 2021). In addition, production and soil amendment with biochar can provide bioenergy and agronomic benefits, and reduce non-CO₂ greenhouse gas

emissions (Lehmann 2007; Woolf et al. 2016; Joseph et al. 2021; Kalu et al. 2022).

Biochar soil application leads to an immediate increase in SOC but how biochar interacts with native and exogenous organic substrates in the long term is not clear. In agricultural soils, exogenous organic substrates such as plant litter, root exudates, and organic amendments are continuously added. Biochar can further increase soil C storage by preserving such exogenous organic substrates and their microbial derivatives from decomposition by promoting strong organo-mineral binding on its surface (Pan et al. 2021; Weng et al. 2022). On the other hand, the addition of exogenous organic substrates such as root exudates can accelerate the mineralization of SOC (priming effect) even when it is strongly bound on

organo-mineral interfaces (Keiluweit et al. 2015), stimulating the loss of both exogenous and native SOC (Fu et al. 2022). Therefore, the potential of biochar for additional soil C sequestration via preservation of new C inputs or reduced priming effects of native SOC depends on complex interactions between biochar, SOC and exogenous organic substrates. How the fresh root exudates (common exogenous organic substrates) in soil-biochar systems simultaneously affect the fate of old-native SOC and the underlying mechanisms remain elusive. The complex interactions and our limited understanding of the associated mechanisms increase the uncertainty to predict long-term C sequestering potential of biochar. One of the important mechanisms controlling the preservation and stabilization of SOC is occlusion within the soil aggregates and sorption onto mineral surfaces (Lehmann and Kleber 2015). Physical fractionation of SOC can provide insights into the mechanistic understanding of the stabilization of fresh and native SOC after biochar amendment.

Priming effect (PE) is a synergistic change in mineralization rates of native SOC following the addition of fresh organic substrate inputs (e.g., fresh plant litter, root exudates or organic amendments) (Kuzakov 2002). Positive PE occurs when exogenous organic substrate inputs stimulate soil microbial activities in a way that accelerates the loss of native SOC (Zhou et al. 2022; Yan et al. 2023). Occasionally, soil microbes can shift their preference from native SOC to easily available fresh organic substrates (substrate switching), leading to the negative PE or retardation of SOC decomposition (Guenet et al. 2010). The change in physico-chemical and microbial properties of soil after biochar application can alter the magnitude and direction of PE. A meta-analysis by Wang et al. (2016) concluded that biochar slightly retarded SOC decomposition by 3.8% compared to soil without biochar. This indicates that biochar can contribute to additional C storage in soil, which if continued for a long time, can in some conditions lead to impressive increases in SOC stocks as demonstrated by the famous Terra Preta soils in Amazonia, which contain 250 Mg ha⁻¹ total organic C (TOC) compared to only 50 Mg ha⁻¹ in adjacent Ferralsols, while only 20% of TOC is covered by biochar (Glaser et al. 2001). However, the magnitude and direction of PE following biochar application in soils can vary depending on the characteristics of biochar, soil and environmental variables (Zimmerman et al. 2011; Fang et al. 2015), making it difficult to predict.

Microbial carbon use efficiency (CUE), defined as the ratio between the amount of C allocated to biosynthesis (new biomass and biological products, including exudates) and the amount of C taken up by microbes (Manzoni et al. 2018), indicates the efficiency with which

microbes convert available organic substrates into stable biosynthesized products (Geyer et al. 2016). High CUE favors the accumulation of SOC storage through increased microbial biomass and by-products or microbial residues, which can be stabilized in soils in the long term (Sinsabaugh et al. 2013; Liang et al. 2017; Tao et al. 2023). High CUE is expected in environments with better nutrient balance and water dynamics (Manzoni et al. 2012). Since biochar reduces soil environmental stress by improving water and nutrient retention, modulating soil pH and providing suitable habitats for the microbes, biochar has the potential to increase microbial CUE (Liu et al. 2020; Pei et al. 2021). But still, the number of studies and our understanding of the linkage between stabilization or depletion of C in biochar-amended soils and CUE are limited (Giagnoni and Renella 2022).

Here, we conducted a soil incubation study for six months with ¹³C labelling technique with the objectives: (1) to explore the effects of biochar on the mineralization of native SOC and added glucose (as a representative of root exudates) in a fine-textured soil and (2) to shed light on mechanistic understanding of how biochar affects the process of stabilization or depletion of SOC and ¹³C-glucose. We addressed the following hypotheses: (1) biochar amendment influences mineralization of SOC (priming effect) and fresh labile organic substrate; (2) the mineralization of SOC and fresh labile organic substrate depends on the amounts of biochar added; (3) biochar facilitates microbial uptake of fresh labile organic substrate and decreases their energy expenditure (lowers respiration), leading to higher CUE; (4) biochar preserves and stabilizes the microbial necromass derived from fresh labile organic substrate after they die.

2 Materials and methods

2.1 Biochar and soil

Biochar was produced from hardwood branches and split. The composition of hardwood species was 80–90% willow (*Salix spp.*), 5–10% birch (*Betula spp.*), and 5–10% of other hardwood species such as alder (*Alnus spp.*), bird cherry (*Prunus padus L.*), and Norway maple (*Acer platanoides L.*). The hardwood feedstock was slowly pyrolyzed using a 0.3 m³ Kon-Tiki kiln. After the pyrolysis, the biochar was soaked with a mixture of tap water and cattle slurry at a ratio of 7:3. The detailed properties of the biochar were presented in Kiani et al. (2021). In brief, the biochar had a pH of 9.9, a total C content of 86%, a total N content of 0.3%, and a specific surface area of 199 m² g⁻¹.

The soil used in this study was fine-textured (silty clay loam with 3% sand, 78% silt, and 19% clay) Endogleyic-Stagnosol (IUSS Working Group WRB 2007) collected from 0–30 cm depth from an agricultural field located in

Hyvinkää (60°35′38.5″N, 24°56′26.3″E) in southern Finland. The soil had a pH of 6.8 and electrical conductivity of 46 $\mu\text{S cm}^{-1}$. The total C and N contents of the soil were 3.7% and 0.3%, respectively.

2.2 Soil incubation

The experiment consisted of six treatments (i) Soil-only, (ii) Soil+B15, (iii) Soil+B30, (iv) Soil+G, (v) Soil+B15+G, and (vi) Soil+B30+G with four replicates. The “B15” and “B30” refer to two rates of biochar applications corresponding to 15 and 30 Mg ha^{-1} in field conditions, respectively and the “G” refers to the addition of ^{13}C -glucose.

After passing the soil through a 4 mm sieve to remove large plant particles and gravel, 41 g fresh soil (=35 g in dry weight basis) was filled in a 120 mL borosilicate glass bottle. Then 0.29 g and 0.58 g of biochar (=0.24 g and 0.48 g dry weight basis) were mixed with soil for the respective B15 and B30 treatments. The glass bottles were closed with a rubber septum and further enclosed with an aluminum crimp cap to ensure airtight condition. Altogether, 168 glass bottles (6 treatments \times 4 replicates \times 7 sets) were first pre-incubated at 15 °C for 78 days at 45% water holding capacity (WHC) to balance out the mineralization and/or priming occurred due to biochar addition. During the pre-incubation, soil respiration was measured continuously, more frequently in the beginning, and sparsely at the end. The purpose of including 7 sets of samples was to take soil samples destructively 7 times during the experiment: on the day of 1, 4, 7, 14, 28, 97, and 180 after ^{13}C -glucose addition.

After the pre-incubation, 15 mg of uniformly labeled ^{13}C -glucose (20 at%) was added per g soil C (the same rate as in Hartley et al. (2010)) into all glucose addition treatments (indicated by “G” in the treatment name). Glucose was added as a solution (3 ml per soil sample), resulting in the final WHC of 60%. In non-labelled treatments, a corresponding amount of Milli-Q water was added to maintain the same WHC. This soil moisture content was maintained throughout the study by periodically checking the weight of the bottle and adding the necessary amount of Milli-Q water.

2.3 Sampling and measurement

2.3.1 CO_2 and $^{13}\text{CO}_2$ production

The CO_2 and $^{13}\text{CO}_2$ production were measured throughout the experiment only from the last set of experimental units, intended for destructive soil sampling 180 days after ^{13}C -glucose addition. During pre-incubation, when ^{13}C -glucose was not yet added, CO_2 production was measured only from 3 treatments—“Soil-only”, “Soil+B15”, and “Soil+B30” on the day of 1, 3, 5, 7, 14, 21, 28, 42 and 78 after biochar addition. For measuring

CO_2 flux at this phase, the bottles were first flushed with ambient air for 1 min followed by enclosing the bottles with airtight caps. Thereafter, using a micro-syringe (Hamilton Co), 100 μL of gas samples were taken from the bottles and inserted into a Gas Chromatograph (GC; Hewlett-Packard—HP 6890 GC System by Agilent Technologies Inc) equipped with a flame ionization detector (FID) for measuring CO_2 concentration at 0, 6 and 24 h after closing the bottles. The CO_2 flux was calculated using linear regression between the CO_2 concentrations and measurement time. On other days when no CO_2 flux was measured, the bottles were closed with ventilation caps for air circulation.

After ^{13}C -glucose addition, CO_2 production was periodically measured from all six treatments from the last set of the experimental units on the day of 0, 1, 2, 3, 4, 5, 6, 7, 11, 14, 19, 50, 68 and 106, while $^{13}\text{CO}_2$ production used to calculate the PE was measured until day 19 only. First, the bottles were enclosed with a rubber septum and aluminum crimp cap followed by flushing with CO_2 -free air at the rate of 1 L min^{-1} for 1 min to remove all the CO_2 present inside the bottle. Then, the bottles were over-pressurized by inserting 7 mL of CO_2 -free air. Consequently, the CO_2 concentrations were measured 6 and 24 h afterward, by introducing 100 μL of gas samples from the bottles to the GC. Right after ^{13}C -glucose addition, higher $^{13}\text{CO}_2$ emissions were expected, therefore, CO_2 concentration was measured only after 6 h. After that, 7 mL of gas sample was taken from the bottle using a syringe and injected into 6 mL evacuated exetainer for measuring $^{13}\text{CO}_2$ production. The gas samples were analyzed for $^{13}\text{CO}_2$ signature using an Isotope Ratio Mass Spectrometer (IRMS; Delta plus XP, Thermo Fisher Scientific, Bremen, Germany) coupled with a Gas Chromatograph (GC-Box, Thermo Fisher Scientific, Bremen, Germany and Poraplot Q, Combi-PAL autosampler, Zwingen, Switzerland) via a ConFlo III Interface (Thermo Fisher Scientific, Bremen, Germany). The amount of CO_2 produced from the mineralization of either added ^{13}C -glucose or native SOC was calculated using the two-pool mixing model (Eqs. 1 and 2), and the PE was calculated using Eq. 3. The cumulative CO_2 or $^{13}\text{CO}_2$ production was calculated through linear interpolation or trapezoidal method.

$$R_{\text{Glucose}} = \frac{^{13}\text{CO}_2 - ^{13}\text{SOC}}{^{13}\text{C}_{\text{Glucose}} - ^{13}\text{C}_{\text{SOC}}} \times R_{\text{Total}} \quad (1)$$

$$R_{\text{SOC}} = R_{\text{Total}} - R_{\text{Glucose}} \quad (2)$$

$$\text{Priming effect} = R_{\text{Trt}} - R_{\text{Ctrl}} \quad (3)$$

where R_{Glucose} is CO_2 derived from the added ^{13}C -glucose; $^{13}\text{CO}_2$ is ^{13}C -at% of sample; ^{13}SOC is ^{13}C -at% of soil, the ^{13}C -at% of soils in the treatments without ^{13}C -glucose (Soil-only, Soil + B15 and Soil + B30) was the same = 1.08; $^{13}\text{C}_{\text{Glucose}}$ is ^{13}C -at% of added ^{13}C -glucose; R_{Total} is the total CO_2 production; R_{SOC} represents CO_2 derived from SOC; R_{Trt} is the CO_2 derived from SOC in a sample treatment and R_{Ctrl} is the CO_2 derived from SOC in the “Soil-only” control treatment.

2.3.2 Soil microbial biomass carbon (MBC) and ^{13}C in microbial biomass

Soil microbial biomass carbon (MBC) was measured on the day of 1, 4, 7, 14, 28, 97 and 180 after ^{13}C -glucose addition using the chloroform fumigation extraction (CFE) method (Vance et al. 1987). For that, 8 g of moist soil samples were fumigated with chloroform inside a desiccator for 24 h in the dark followed by their extraction with 40 mL 0.05 M K_2SO_4 by shaking on an orbital shaker (200 rpm, 30 min). The extracts were filtered using Whatman Grade 42 ashless filter paper and subsequently filtered through a 0.45 μm syringe filter (Sartorius, Minisart High Flow, PES). At the same time, another soil sample without fumigation was also extracted similarly. The extracts were then analyzed for dissolved organic C (DOC) using a TOC analyzer (Analytik Jena multi N/C 3100, Jena, Germany). The MBC was calculated by subtracting the DOC of the non-fumigated extract (NF) from the fumigated extract (F).

The K_2SO_4 extracts of samples obtained on the day of 1, 14, and 180 were freeze-dried followed by ^{13}C analysis using an IRMS (Delta C, Thermo Electron, Bremen, Germany) coupled with an Elemental Analyzer (Costech ECS 4010, Costech Analytical Technologies Inc., Valencia, USA) via a Conflo III Interface (Thermo Electron, Bremen, Germany). The ^{13}C in the microbial biomass (^{13}MBC) and microbial carbon use efficiency (CUE) of ^{13}C -glucose were calculated using Eqs. 4–7 as in Mganga et al. (2022). The CUE was calculated for the day of 1 and 14 after the ^{13}C -glucose addition.

$$^{13}\text{MBC}_x = \frac{^{13}\text{DOC}_F \times \text{DOC}_F - ^{13}\text{DOC}_{\text{NF}} \times \text{DOC}_{\text{NF}}}{\text{DOC}_F - \text{DOC}_{\text{NF}}} \quad (4)$$

$$^{13}\text{MBC}\% = \frac{^{13}\text{MBC}_T - ^{13}\text{MBC}_C}{^{13}\text{Glucose} - ^{13}\text{MBC}_C} \times 100 \quad (5)$$

$$^{13}\text{MBC} = (\text{DOC}_F - \text{DOC}_{\text{NF}}) \times \frac{^{13}\text{MBC}\%}{100} \quad (6)$$

$$\text{CUE} = \frac{^{13}\text{MBC}}{^{13}\text{MBC} + R_{\text{Glucose}}} \quad (7)$$

where $^{13}\text{MBC}_x$ represents either $^{13}\text{MBC}_T$ or $^{13}\text{MBC}_C$ in Eq. (5); $^{13}\text{DOC}_F$, DOC_F , $^{13}\text{DOC}_{\text{NF}}$, and DOC_{NF} represent the ^{13}C -at% and total C concentrations (mg C kg^{-1} soil) of fumigated (F) and non-fumigated (NF) K_2SO_4 extracts, respectively. $^{13}\text{MBC}_T$ and $^{13}\text{MBC}_C$ (denoted as $^{13}\text{MBC}_x$ in Eq. 4) are the ^{13}C -at% of sample treatments and the control (Soil-only treatment), respectively; $^{13}\text{Glucose}$ is the ^{13}C -at% of added ^{13}C -glucose solution (20 at%). ^{13}MBC is total microbial growth derived from added ^{13}C -glucose and R_{Glucose} is the cumulative respiration derived from added ^{13}C -glucose.

2.3.3 Soil density fractionation

The remaining soil samples from the 180 day samples were dried at 60 °C for 72 h and stored in room temperature until processed for the fractionation into free-particulate (f-POM), occluded-particulate (o-POM), and mineral-associated organic matter (MAOM) according to methods mentioned in Weng et al. (2017) with slight modification. For the fractionation, about 10 g of dry soil samples were added with 40 mL of 1.85 g cm^{-3} sodium polytungstate (SPT) solution in a centrifuge tube. After gently inverting the soil SPT mixtures 10 times, it was centrifuged at 2000 g for 1 h. Then, the floating particles were filtered using 45 μm pore-sized filter paper (GN-6 Metrical® membrane, Pall membrane filters), washed with 100 mL of Milli-Q water to remove the SPT solution and dried at 60 °C until the weight remained constant for 24 h. This fraction is the f-POM.

The remaining soil in the centrifuge tube was washed by adding 40 mL of Milli-Q water, centrifuged at 2000 g for 30 min and discarding the supernatant. This process was repeated 5 times to remove all the SPT. After washing, 40 mL of Milli-Q water was added on top of the decanted sample along with 6 glass beads. The mixture was shaken in an orbital shaker overnight (18 h at 250 rpm) to break all the aggregates. Afterward, the mixture was passed through a 63 μm sieve. The fraction retained on the sieve was the o-POM and the one passing through the sieve was MAOM. These fractions were transferred to the pre-weighed aluminum tray and dried at 60 °C until the weight remained constant for 24 h.

These fractions as well as bulk soil were grinded using a mortar and pestle and then analyzed for C and ^{13}C contents using the IRMS (Delta C, Thermo Electron, Bremen, Germany) coupled with the Elemental Analyzer (Costech ECS 4010, Costech Analytical Technologies Inc., Valencia, USA) via the Conflo III Interface (Thermo Electron, Bremen, Germany). The amount of ^{13}C remained after 6 months (180 days) in the bulk soil, and the different density fractions (f-POM, o-POM, MAOM) were calculated using the two-pool mixing model, similarly as in Eq. (1).

2.3.4 Extraction of amino sugars

The soil amino sugar fractions were extracted from samples destructively sampled at the end of the experiment (180 days) from three treatments “Soil-only”, “Soil+G” and “Soil+B30+G”. In addition, the biochar particles recovered from “Soil+B30” and “Soil+B30+G” treatments were extracted for amino sugars (biochar particles had to be pooled from different analytical replicates to extract enough amino sugars for the ^{13}C analysis). For determination of ^{13}C in total amino sugar fraction, grinded biochar particles or soil(+biochar mixtures) were hydrolyzed with 6 M HCl as described by Dippold et al. (2014), and purified through cation-exchange columns (Poly-Prep[®] Columns, AG[®] 50W-X8, hydrogen form mesh size 100–200; Biorad, Munich, Germany, Cat# 731–6213), in order to remove hydrolyzable cationic compounds such as carboxylic acids and inorganic cations such as iron and aluminum. The ^{13}C in total amino sugar fraction was measured using a EURO EA Elemental Analyzer (EuroVector, Hekatech, Germany) coupled via a ConFlo III Interface to an IRMS (Finnigan Delta V Advantage, Thermo Scientific, Bremen, Germany). Sucrose (ANU, IAEA, Vienna, Austria) and CaCO_3 (NBS 19, TS limestone) were used as calibration standards. The precision of ^{13}C measurements was 0.2‰.

2.4 Data analysis

The differences in treatments were analyzed using one-way analysis of variance (ANOVA) followed by the least significant difference (LSD) test to test the significant differences between the treatments ($P < 0.05$). The assumptions of normality and homogeneity of variances were tested using the Shapiro–Wilk test and Levene’s test. The Shapiro–Wilk test was carried out on the residuals of ANOVA for testing the normality. All the results shown

represent the average of the four replicates ($n = 4$) \pm standard error (SE). The analyses were performed in R Statistical Software v4.2.2 (R Core Team 2022).

3 Results

3.1 CO_2 production

During the pre-incubation, CO_2 production rapidly increased immediately after the addition of biochar and was proportional to the biochar application rate (Fig. 1). However, only after a few days, CO_2 production rates from biochar treatments sharply decreased and were even lower than the control soil without biochar. This trend continued during the entire pre-incubation period of 78 days, indicating that biochar addition significantly reduced the mineralization of native SOC or negative PE. At the end of the pre-incubation, cumulative CO_2 productions from biochar-amended soils were 20% to 36% less than in the Soil-only control.

After glucose addition, CO_2 production rapidly increased for a short period and peaked within 3 days in all glucose-added treatments (Fig. 2). Among them, the treatments with glucose added to biochar-amended soil had significantly lower CO_2 production compared to the treatment with glucose added to soil without biochar. There was also a clear effect of biochar amount, i.e., more biochar addition resulted in less CO_2 production. The trend in the total CO_2 production in treatments without glucose addition was the same as during the pre-incubation i.e., Soil-only > Soil+B15 > Soil+B30.

Likewise, the production of CO_2 derived from SOC and glucose among the glucose-added treatments followed the same trend as the total CO_2 production (Figs. 3 and 4) i.e., Soil+G > Soil+B15+G > Soil+B30+G. The addition of glucose led to immediate positive priming in all three treatments amended with

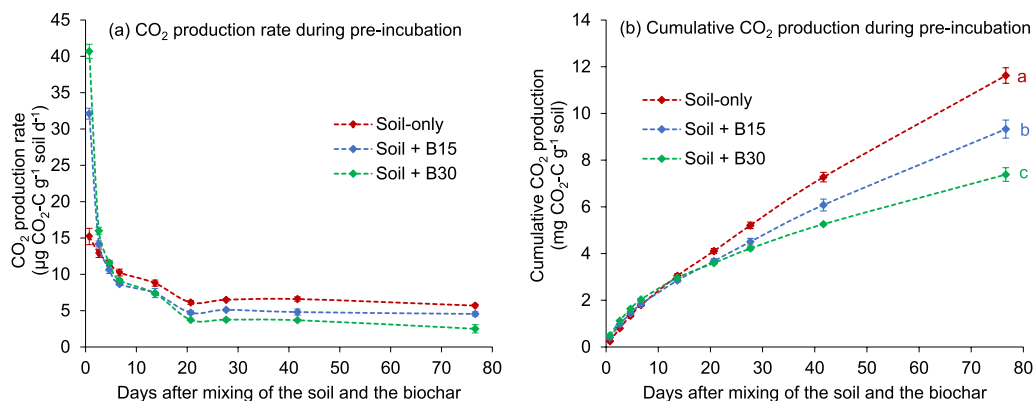


Fig. 1 **a** CO_2 production rate and **b** cumulative CO_2 production after the addition of biochar between the treatments during the pre-incubation. The figure presents the average of the four replicates ($n = 4$) and the error bars represent SE. Different lowercase letters in **b** represent the significant differences in total cumulative CO_2 production between the treatments ($P < 0.05$)

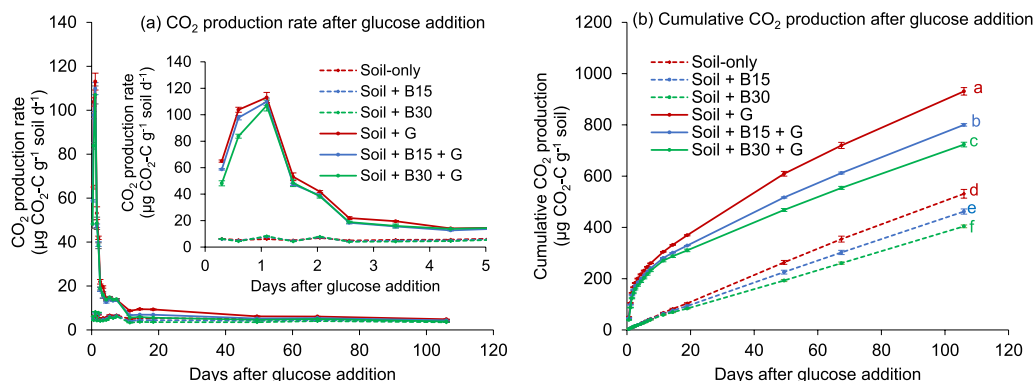


Fig. 2 a CO₂ production rate and b cumulative CO₂ production after glucose addition between the treatments. The figure presents the average of the four replicates (n=4) and the error bars represent SE. Different lowercase letters in b represent the significant differences in total cumulative CO₂ production between the treatments (*P* < 0.05)

glucose. However, after 12 days, the mineralization of SOC decreased in biochar-added treatments leading to negative PE, while the Soil+G treatment continued to exhibit positive PE (Fig. 3c). Compared to the Soil+G control, Soil+B15+G and Soil+B30+G treatments had 12% and 15% less cumulative CO₂ production derived from SOC, respectively. There was no significant difference between the Soil+B15+G and Soil+B30+G treatments on the production of CO₂ derived from SOC (Fig. 3b).

Similarly, the biochar treatments (Soil+B15+G and Soil+B30+G) significantly decreased the production of ¹³CO₂ derived from glucose compared to the Soil+G treatment (*P* < 0.05) (Fig. 4b). The higher the biochar application rate, the lower the mineralization of added glucose. The most significant reduction in glucose mineralization by the biochar occurred immediately after the addition (on Days 1 and 3; Fig. 4a). Compared to the Soil+G control, Soil+B15+G and Soil+B30+G treatments had 11% and 17% less cumulative CO₂ production

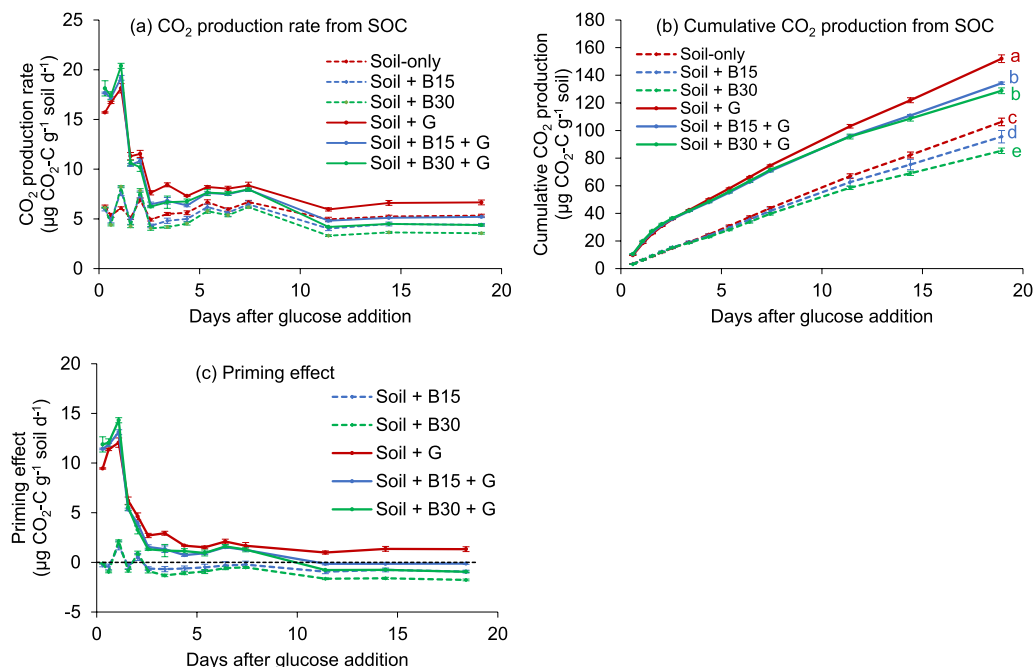


Fig. 3 a CO₂ production rate originating from SOC decomposition, b cumulative CO₂ production derived from SOC, and c priming effect between the treatments. The figure presents the average of the four replicates (n=4) and the error bars represent SE. Different lowercase letters in b represent the significant differences in total cumulative CO₂ production derived from SOC between the treatments (*P* < 0.05)

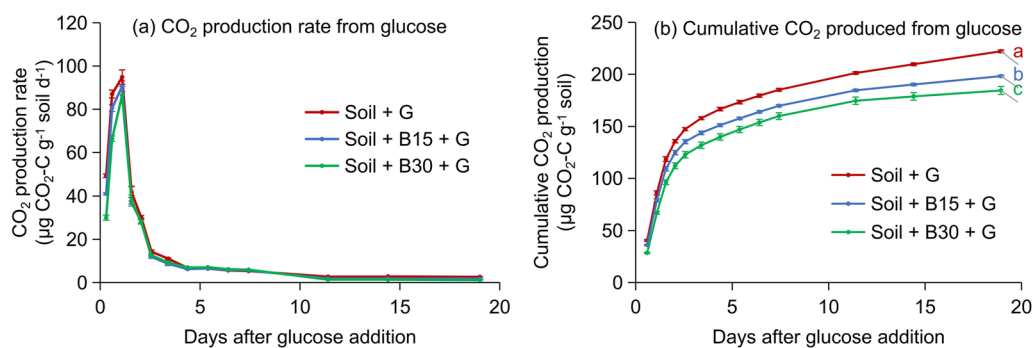


Fig. 4 **a** CO₂ production rate and **b** cumulative CO₂ production originated from glucose between the treatments. The figure presents the average of the four replicates (n=4) and the error bars represent SE. Different lowercase letters in **b** represent the significant differences in total cumulative CO₂ production derived from glucose between the treatments (*P*<0.05)

derived from added glucose, respectively (Fig. 4b). After 19 days, 32–35% of the added glucose had been mineralized in the biochar treatments, whereas 39% of the added glucose had been mineralized in the control treatment.

3.2 Microbial biomass carbon and carbon use efficiency

Biochar treatments with glucose addition (Soil+B15+G and Soil+B30+G) had significantly higher MBC than other treatments throughout the 180 days of incubation (Fig. 5a). However, there was no difference in MBC between the Soil+B15+G and Soil+B30+G treatments. Also, no statistically significant effect of biochar was observed on ¹³MBC although the average values were slightly higher in the biochar treatments than in the Soil+G treatment throughout the experiment (Fig. 5b).

Biochar addition increased microbial CUE. Greater CUE was found in the higher biochar application rate treatment (Fig. 6). On day 1, the greater variance in ¹³MBC (Fig. 5b) resulted in greater variance in CUE, constraining the statistical significance (*P*>0.05). However, on day 14, the Soil+B30+G had significantly higher CUE than the Soil-only control (*P*<0.05).

3.3 Partitioning of soil C in different fractions

After 6 months, biochar-amended soils had significantly higher soil C content than the Soil-only control (*P*<0.05). The 15 Mg ha⁻¹ biochar treatments (Soil+B15 and Soil+B15+G) had 20% and 30 Mg ha⁻¹ biochar treatments (Soil+B30 and Soil+B30+G) had 32% higher total soil C content compared to the Soil-only control (Fig. 7a). After 6 months, about 29–30% of the ¹³C label remained in glucose-amended soils. The percentage of ¹³C remaining in Soil+B30+G treatment was slightly higher but not statistically significant (*P*>0.05) than Soil-only and Soil+B15+G treatments (Fig. 7b).

Soil fractionation revealed that most of the soil mass (88–90%; Fig. 8) and the remaining ¹³C (about 22% out of 29–30% of remaining ¹³C; Fig. 9) were recovered in mineral-associated fraction (MAOM). Most of the biochar particles were recovered in the f-POM fraction because biochar-amended soils had significantly higher (*P*<0.05) mass of f-POM fraction than the Soil-only and Soil+G treatments (Fig. 8). Also, the mass of o-POM fraction was significantly higher (*P*<0.05) in biochar treatments (2.8% and 2.6% in Soil+B15 and Soil+B30 treatments, respectively) compared to the Soil-only treatment (2.1%),

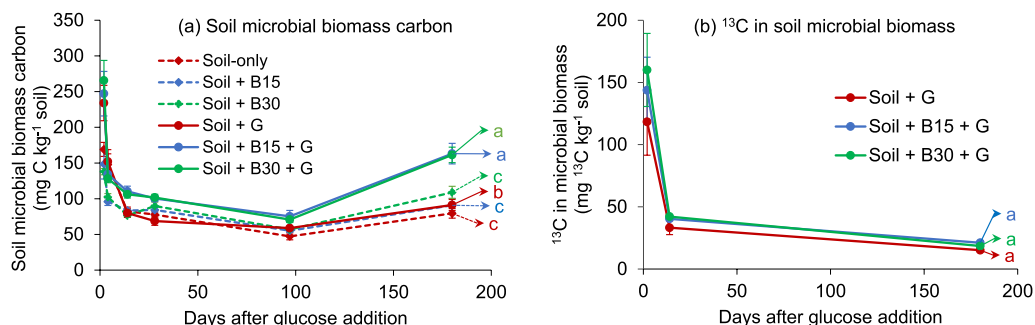


Fig. 5 **a** Soil microbial biomass carbon (MBC) and **b** ¹³C in microbial biomass (¹³MBC) between the treatments over 180 days of the incubation. The figure presents the average of the four replicates (n=4) and the error bars represent SE. Different lowercase letters represent the significant differences between the overall average of the treatments (*P*<0.05)

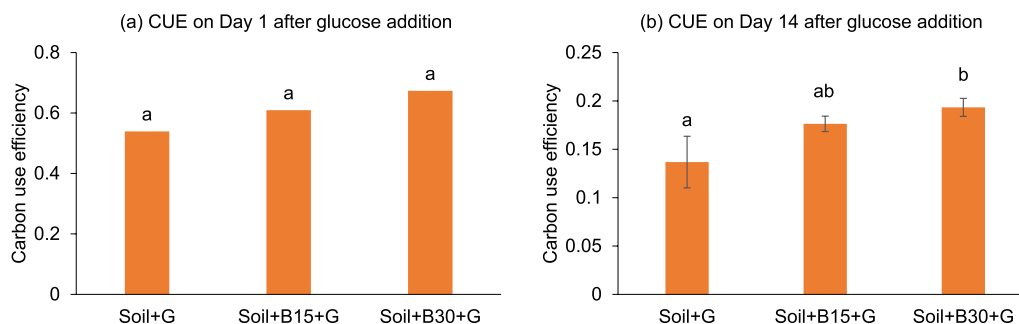


Fig. 6 Microbial carbon use efficiency (CUE) of glucose in ¹³C-glucose-amended treatments on (a) Day 1 and (b) Day 14 after ¹³C-glucose addition. The figure presents the average of the four replicates (n=4) and the error bars represent SE; no error bars are shown for **a** because of the large SE. Different lowercase letters represent the significant differences between the treatments (P<0.05)

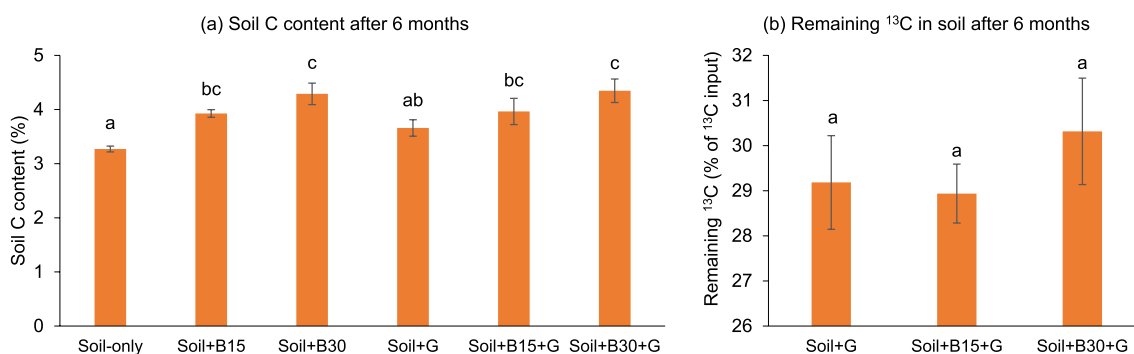


Fig. 7 a Soil C contents and b remaining ¹³C in soil after 6 months of the experiment. The percentage in (b) represents the percentage of added ¹³C-glucose. The figure presents the average of the four replicates (n=4) and error bars represent SE. Different lowercase letters represent the significant differences between the treatments (P<0.05)

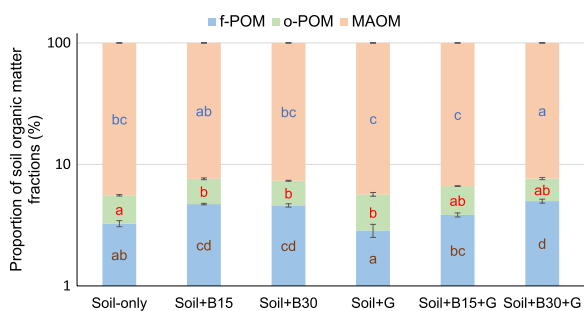


Fig. 8 Proportion of different soil organic matter fractions (f-POM, o-POM, and MAOM) after 6 months of incubation. The y-axis is in logarithmic scale. The figure presents the average of the four replicates (n=4) and the error bar represents SE. Different lowercase letters represent the significant differences between the treatments (P<0.05)

particularly in treatments without glucose addition (Fig. 8), indicating that biochar increased soil occlusion or aggregation in non-glucose amended treatments.

The ¹³C contents in the soil fractions showed a significantly higher (P<0.05) amount of ¹³C remaining in the f-POM fraction in the biochar treatments (1.3%

and 1.8% of added ¹³C remaining in Soil+B15+G and Soil+B30+G treatments) than in the Soil+G treatment (0.7%) after 6 months (Fig. 9). However, no differences in the remaining ¹³C were found between the treatments in o-POM and MAOM fractions.

3.4 Amino sugars

Soil amended with biochar (Soil+B30+G) had significantly higher total amino sugar C and ¹³C amino sugar contents than controls (Soil-only and Soil+G treatments) (P<0.05) (Table 1). In addition, ¹³C at% of amino sugar measured from biochar particles collected from the treatment receiving ¹³C-glucose (Soil+B30+G) was higher compared to that of soil from Soil+G or Soil+B30+G treatments indicating that dead microbial residues derived from consuming ¹³C-glucose were concentrated on biochar particles. The percentage of ¹³C in amino sugars (percentage of the total ¹³C remaining in the soil at the end of the incubation) was on average 10.8% in the Soil+G treatment and 11.2% in the Soil+B30+G. Our results indicated that ¹³C of added glucose was incorporated into soil microorganisms and

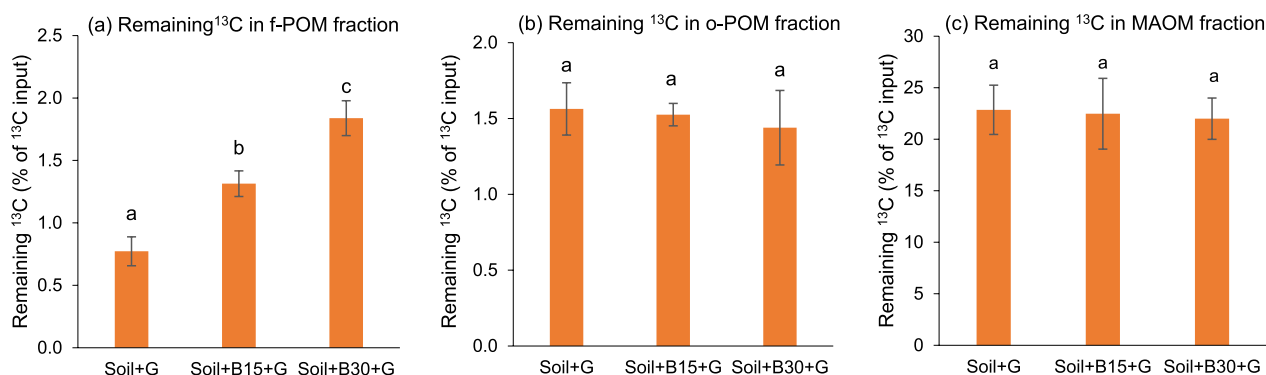


Fig. 9 Recovery of added ¹³C in different soil fractions among the ¹³C-glucose-added treatments after 6 months. The figure presents the average of the four replicates (n=4) and the error bars represent SE. Different lowercase letters represent the significant differences between the treatments (P < 0.05)

Table 1 Total amino sugar C and ¹³C amino sugar contents of soil and biochar particles at different treatments

Treatment	Soil			Biochar		
	Total amino sugar C (mg C g ⁻¹ soil)	¹³ C at% of amino sugar	¹³ C amino sugar (µg C g ⁻¹ soil)	Total amino sugar C (mg C g ⁻¹ biochar)	¹³ C at% of amino sugar	¹³ C amino sugar (µg C g ⁻¹ biochar)
Soil-only	1.26 a	1.08 a	13.57 a			
Soil+G	1.35 a	1.25 b	16.85 b			
Soil+B30	–	–	–	1.03	1.08	11.11
Soil+B30+G	1.54 b	1.24 b	19.02 c	1.15	1.38	15.89
LSD	0.17	0.03	1.91			

Different letters within columns indicate significant differences between treatments (P < 0.05). For biochar particles, samples from 4 replicates had to be pooled for analysis (n = 1)

stabilized in biochar pores as microbial necromass, i.e., in the form of amino sugars.

4 Discussion

4.1 Biochar reduced SOC mineralization: negative priming

Immediately after the addition, biochar increased CO₂ production for one week (Fig. 1a). This immediate short-term increase in CO₂ production after biochar addition is common and mainly attributed to the presence of labile C fraction in biochar, which fuels the microbes in the short term (Maestrini et al. 2015). Previous studies also observed increased short-term mineralization of SOC immediately after biochar addition, but this positive priming decreased over time (Luo et al. 2013; Singh and Cowie 2014). However, similar ¹³C signatures of soil and biochar in this study did not allow us to separate the proportion from which this CO₂ production originated (soil or biochar). Nevertheless, it was evident that after one week, biochar decreased the mineralization of native SOC, i.e., negative priming of native SOC occurred for the rest of the pre-incubation period. This result shows that biochar-induced positive priming is short-lived

followed by negative priming (Zimmerman et al. 2011; Maestrini et al. 2015; Weng et al. 2015).

The addition of easily mineralizable glucose indeed induced short-term positive PE from the soil-biochar system for 12 days (Fig. 3c). This is linked to the immediate microbial blooming (Fig. 5a). However, in the longer term (after 12 days of glucose addition), added biochar reduced SOC mineralization i.e., negative PE of native SOM occurred. This biochar-induced negative PE could arguably be explained by an increase in soil occlusion or aggregation by the biochar, as indicated by increased o-POM in the biochar treatments (Fig. 8). Our results conform to a previous study, which also observed an increase in soil aggregate stability when the same soil used in this experiment was amended with a wood-based biochar (Soenne et al. 2014). The binding of soil organic and mineral components at the large surface area of biochar increases inter-particle cohesion, which is the primary step in the aggregate formation and stabilization process (Gul et al. 2015). The increase in soil aggregation by biochar protects the native SOC from microbial degradation (Weng et al. 2017; Fang et al. 2018).

Substrate switching and dilution effects (preference of the microbes to decompose labile biochar C and other easily mineralizable substrates over native SOC because of biochar) are the other possible mechanisms behind biochar-induced negative priming (Joseph et al. 2021). However, such mechanisms usually result in the transient negative priming immediately after the substrate or biochar addition, followed by a positive priming (Whitman et al. 2014), which was not observed in this study. In some cases, biochar might decrease microbial biomass (Dempster et al. 2012) that could lead to negative priming. On the contrary, MBC increased especially in the glucose-added biochar treatments in this study. Hence, physical protection of SOC due to increased soil aggregation and/or sorption of labile native SOC into the biochar porous matrix seems plausible mechanisms behind the observed negative PE.

4.2 Biochar particles retained added ^{13}C

Most of the biochar particles were recovered in f-POM fraction. The significantly higher recovery of added ^{13}C in f-POM fraction of biochar treatments (Fig. 9a) denotes that the added ^{13}C was recovered in biochar particles. This demonstrates the additional preservation of labile organic substrates (e.g., root exudates) inside or in close proximity to biochar particles (charosphere region). This increased recovery of ^{13}C in biochar particles could be due to the physico-chemical sorption or via microbial pathways. The physico-chemical sorption of added glucose in biochar particles occurs mostly immediately after the addition of glucose (Melas et al. 2017). However, in the longer term, part or most of the added glucose would have been desorbed and consumed by soil microorganisms. Our results agree with the concept that biochar usually benefits microbial growth and activity because of the supply of labile C present in biochar (Luo et al. 2013; Farrell et al. 2013) as well as serving as the preferred microbial habitat in its large and porous surface matrix (Pietikäinen et al. 2000; Lehmann et al. 2011). The increased microbial biomass and CUE of glucose in biochar-amended soil (especially in the higher biochar application rate treatments) suggest that the added glucose might have been effectively and/or preferentially used by soil microorganisms to synthesize new biomass. This is supported by the increased ^{13}MBC in biochar-amended soils at the beginning of the experiment (Fig. 5b; although not statistically significant). Eventually, ^{13}C in microbial biomass was converted to microbial byproducts (microbial necromass and metabolites).

Biochar facilitated stable microbial necromass formation from the added labile C substrate, as indicated by the higher recovery of ^{13}C in amino sugar by biochar (Table 1). In agreement with our result, some previous

studies also suggested that biochar can enhance microbial necromass (Glaser and Birk 2012; Weng et al. 2022; Zhang et al. 2022). Higher accumulation of ^{13}C into amino sugars (microbial necromass) also indicates a higher capacity to store SOC in rather stable forms in biochar-amended soils (Zhu et al. 2020). Microbial necromass is sticky in nature (Dufréne 2015; Buckeridge et al. 2020) and could strongly adsorb on biochar, hence increasing the long-term CUE and thus ^{13}C retention in biochar particles. The CUE measured after 14 days in this study can be considered ecosystem level CUE, which measures not only the effective uptake of ^{13}C -glucose to synthesize microbial biomass but also includes the efficiency of the substrate (microbial necromass and exudates) recycling, and stabilization in soil (Geyer et al. 2016). Microbial CUE indicates the microbial C sequestration potential in soils because it compares microbial decomposition of organic substrate and stabilization of microbially assimilated C (Manzoni et al. 2018). In our study, biochar enhanced CUE because biochar reduced the mineralization of ^{13}C glucose, while increasing the proportion of microbially assimilated C, and its stabilization as microbial necromass. Greater CUE also indicates that biochar reduced environmental stress to microbes by regulating soil pH (Pei et al. 2021) and providing nutrient supply (Liu et al. 2020).

Previous studies suggested that biochar increases organo-mineral interaction and thus enhances the retention of (labile) organic matter in MAOM (Weng et al. 2017; Akpınar et al. 2023; Gianetta et al. 2023; Zhang et al. 2023). Biochar did not increase the amount of SOC stabilized in the MAOM fraction in this study (Fig. 9c). A probable explanation for this observation is that the tightly held organo-mineral layer, formed on the biochar surface after its prolonged exposure to soil (Hagemann et al. 2017), was probably not easily disintegrated into the solution when dispersed in SPT during density fractionation. Yet, the density of biochar with the organo-mineral layer was still lower than 1.85 g cm^{-3} SPT, hence, it was recovered in the f-POM fraction. Because more clay minerals attached to biochar particles could have been recovered in f-POM fraction in the treatments with high biochar application rate, the mass of clay mineral-dominated MAOM fraction in the higher biochar application rate treatment (Soil+B30+G) was significantly lower than in the Soil+G treatment (Fig. 8). Interestingly, this significant difference was only observed in glucose-amended treatments. This suggests that glucose or glucose-derived microbial metabolites might have increased the interaction of biochar and clay minerals. In this organo-mineral-biochar interface, multivalent cations from soil minerals can bridge negatively charged functional groups of organic molecules originating either

from SOC or newly added organic substrate or their microbial derivatives on one side, and negatively charged biochar surface on the other (Weng et al. 2022).

The retention of added labile organic substrate or its microbial derivatives by the biochar was relatively small. For instance, the retention of ^{13}C in f-POM in Soil + G control was 0.7% whereas that in the biochar treatments: Soil + B15 + G, and Soil + B30 + G treatments were 1.3% and 1.8% of the added ^{13}C , respectively, after 6 months (Fig. 9a). Similarly, the retentions of ^{13}C amino sugars in the Soil + G control and Soil + B30 + G treatments were 10.8% and 11.2% of the total ^{13}C retained, respectively. Nevertheless, the ability of the biochar to retain the added labile organic substrate and its microbial derivatives could be expected to be additive over time under field conditions, where plants continuously release root exudates in the soil (Joseph et al. 2021; Weng et al. 2022). Even though this study was limited to only one soil and biochar type, it does provide evidence for (1) the reduction of SOC mineralization and (2) efficient microbial utilization of added labile substrate in the presence of biochar and (3) eventual protection or stabilization of added labile substrate inside biochar particles as microbial necromass, which helps in promoting soil C sequestration. However, extrapolation of our results with a simple soil-biochar and glucose system from a controlled environment at constant temperature and moisture content to wider fields with complex organic inputs (e.g. other soil amendments, plant litter) should be considered cautiously. Further experiments under field conditions with different organic substrate inputs, soil and biochar types will improve our understanding of the key factors affecting mineralization of fresh and added SOC dynamics after soil biochar application.

5 Conclusions

Biochar reduced the mineralization of SOC by 12–15% and added glucose by 11–17%. Our results demonstrated the additional soil C storage ability of wood-based biochar by preserving SOC from mineralization (negative priming) and stabilizing fresh labile substrate. The higher application rate of biochar (30 Mg ha⁻¹) has higher soil C sequestration potential aided with increased negative priming and increased retention of added labile organic substrate. The inaccessibility of SOC to the microbes due to increased soil occlusion in the biochar-amended soil preserved SOC from mineralization. Similarly, biochar increased microbial CUE, suggesting that biochar helped in the effective conversion of labile organic substrate to stable microbial products. Furthermore, ^{13}C amino sugar analysis of biochar particles confirmed that microbial necromass derived from the labile organic substrate was stabilized inside

biochar's porous matrix. Over the long run, conversion and stabilization of fresh labile organic substrate into microbial necromass by biochar could be a way to form a greater fraction of stable SOC.

Acknowledgements

We would like to thank Priit Tammeorg for providing biochar for this study. The Centre for Stable Isotope Research and Analysis, University of Göttingen, Germany is acknowledged for measuring ^{13}C contents of the samples. Thanks to Heike Maennicke, Tobias Bromm, and Marianne Zech for ^{13}C amino sugar analysis.

Author contributions

SK and KK planned the experiment. SK conducted the experiment. AS, OMS and KM assisted in lab work. BG analyzed the ^{13}C content of total amino sugar fractions. SK conducted data analysis and prepared manuscript draft. All the co-authors commented on the manuscript.

Funding

This study was funded by the University of Helsinki three-year Grant (Decision number HY/66/05.01.07/2017), Helsinki Institute of Life Science (HiLIFE Fellow grant to KK), and Academy of Finland (Grant number 316401).

Availability of data and materials

Data will be shared upon reasonable request.

Declarations

Competing interests

The authors do not have any competing interests.

Author details

¹Faculty of Agriculture and Forestry, University of Helsinki, Helsinki, Finland. ²Helsinki Institute of Sustainability Science (HELSUS), Helsinki, Finland. ³Department of Crop and Soil Sciences, North Carolina State University, Raleigh, USA. ⁴Copernicus Institute of Sustainable Development, Utrecht University, Utrecht, The Netherlands. ⁵HAMK Bio Research Unit, Häme University of Applied Sciences, Hämeenlinna, Finland. ⁶Institute of Agricultural and Nutritional Sciences, Department of Soil Biogeochemistry, Martin Luther University Halle-Wittenberg, Halle, Germany. ⁷Helsinki Institute of Life Science (HiLIFE), Helsinki, Finland.

Received: 14 July 2023 Revised: 28 November 2023 Accepted: 30 November 2023

Published online: 15 January 2024

References

- Akpınar D, Tian J, Shepherd E, Imhoff PT (2023) Impact of wood-derived biochar on the hydrologic performance of bioretention media: effects on aggregation, root growth, and water retention. *J Environ Manage* 339:117864. <https://doi.org/10.1016/j.jenvman.2023.117864>
- Buckeridge KM, La Rosa AF, Mason KE, Whitaker J, McNamara NP, Grant HK, Ostle NJ (2020) Sticky dead microbes: rapid abiotic retention of microbial necromass in soil. *Soil Biol Biochem* 149:107929. <https://doi.org/10.1016/j.soilbio.2020.107929>
- Dempster DN, Gleeson DB, Solaiman ZM, Jones DL, Murphy DV (2012) Decreased soil microbial biomass and nitrogen mineralisation with Eucalyptus biochar addition to a coarse textured soil. *Plant Soil* 354:311–324. <https://doi.org/10.1007/s11104-011-1067-5>
- Dippold MA, Boesel S, Gunina A, Kuzyakov Y, Glaser B (2014) Improved $\delta^{13}\text{C}$ analysis of amino sugars in soil by ion chromatography–oxidation–isotope ratio mass spectrometry. *Rapid Commun Mass Spectrom* 28:569–576. <https://doi.org/10.1002/rcm.6814>
- Duffrène YF (2015) Sticky microbes: forces in microbial cell adhesion. *Trends Microbiol* 23:376–382. <https://doi.org/10.1016/j.tim.2015.01.011>

- Fang Y, Singh B, Singh BP (2015) Effect of temperature on biochar priming effects and its stability in soils. *Soil Biol Biochem* 80:136–145. <https://doi.org/10.1016/j.soilbio.2014.10.006>
- Fang Y, Singh BP, Luo Y, Boersma M, Van Zwieten L (2018) Biochar carbon dynamics in physically separated fractions and microbial use efficiency in contrasting soils under temperate pastures. *Soil Biol Biochem* 116:399–409. <https://doi.org/10.1016/j.soilbio.2017.10.042>
- Farrell M, Kuhn TK, Macdonald LM, Maddern TM, Murphy DV, Hall PA, Singh BP, Baumann K, Krull ES, Baldock JA (2013) Microbial utilisation of biochar-derived carbon. *Sci Tot Environ* 465:288–297. <https://doi.org/10.1016/j.scitotenv.2013.03.090>
- Field CB, Mach KJ (2017) Rightsizing carbon dioxide removal. *Science* 356:706–707. <https://doi.org/10.1126/science.aam9726>
- Fu Y, Luo Y, Auwal M, Singh BP, Van Zwieten L, Xu J (2022) Biochar accelerates soil organic carbon mineralization via rhizodeposit-activated Actinobacteria. *Biol Fertil Soils* 58:565–577. <https://doi.org/10.1007/s00374-022-01643-y>
- Geyer KM, Kyker-Snowman E, Grandy AS, Frey SD (2016) Microbial carbon use efficiency: accounting for population, community, and ecosystem-scale controls over the fate of metabolized organic matter. *Biogeochemistry* 127:173–188. <https://doi.org/10.1007/s10533-016-0191-y>
- Giagnoni L, Renella G (2022) Effects of biochar on the C use efficiency of soil microbial communities: components and mechanisms. *Environments* 9:138. <https://doi.org/10.3390/environments9110138>
- Giannetta B, Plaza C, Cassetta M, Mariotto G, Benavente-Ferraces I, García-Gil JC, Panettieri M, Zaccone C (2023) The effects of biochar on soil organic matter pools are not influenced by climate change. *J Environ Manage* 341:118092. <https://doi.org/10.1016/j.jenvman.2023.118092>
- Glaser B, Birk JJ (2012) State of the scientific knowledge on properties and genesis of Anthropogenic Dark Earths in Central Amazonia (terra preta de índio). *Geochim Cosmochim Acta* 82:39–51. <https://doi.org/10.1016/j.gca.2010.11.029>
- Glaser B, Haumaier L, Guggenberger G, Zech W (2001) The ‘Terra Preta’ phenomenon: a model for sustainable agriculture in the humid tropics. *Naturwissenschaften* 88:37–41. <https://doi.org/10.1007/s001140000193>
- Gross A, Bromm T, Glaser B (2021) Soil organic carbon sequestration after biochar application: a global meta-analysis. *Agronomy* 11:2474. <https://doi.org/10.3390/agronomy11122474>
- Guenet B, Leloup J, Raynaud X, Bardoux G, Abbadie L (2010) Negative priming effect on mineralization in a soil free of vegetation for 80 years. *Eur J Soil Sci* 61:384–391. <https://doi.org/10.1111/j.1365-2389.2010.01234.x>
- Gul S, Whalen JK, Thomas BW, Sachdeva V, Deng H (2015) Physico-chemical properties and microbial responses in biochar-amended soils: mechanisms and future directions. *Agri Ecosyst Environ* 206:46–59. <https://doi.org/10.1016/j.agee.2015.03.015>
- Hagemann N, Joseph S, Schmidt H-P, Kammann CI, Harter J, Borch T, Young RB, Varga K, Taherymoosavi S, Elliott KW, McKenna A, Albu M, Mayrhofer C, Obst M, Conte P, Dieguez-Alonso A, Orsetti S, Subdiaga E, Behrens S, Kappler A (2017) Organic coating on biochar explains its nutrient retention and stimulation of soil fertility. *Nat Commun* 8:1089. <https://doi.org/10.1038/s41467-017-01123-0>
- Hartley IP, Hopkins DW, Sommerkorn M, Wookey PA (2010) The response of organic matter mineralisation to nutrient and substrate additions in sub-arctic soils. *Soil Biol Biochem* 42:92–100. <https://doi.org/10.1016/j.soilbio.2009.10.004>
- IPCC (2022) Climate change 2022: Mitigation of climate change. Working group III contribution to the sixth assessment report of the Intergovernmental Panel on Climate Change
- IUSS Working Group WRB (2007) World reference base for soil resources, first update. World Soil Resources Report 103
- Joseph S, Cowie AL, Van Zwieten L, Bolan N, Budai A, Buss W, Cayuela ML, Graber ER, Ippolito JA, Kuzyakov Y, Luo Y, Ok YS, Palansooriya KN, Shepherd J, Stephens S, Weng Z, Lehmann J (2021) How biochar works, and when it doesn't: a review of mechanisms controlling soil and plant responses to biochar. *GCB Bioenergy* 13:1731–1764. <https://doi.org/10.1111/gcbb.12885>
- Kalu S, Kulmala L, Zrim J, Peltokangas K, Tammeorg P, Rasa K, Kitzler B, Pihlatie M, Karhu K (2022) Potential of biochar to reduce greenhouse gas emissions and increase nitrogen use efficiency in boreal arable soils in the long-term. *Front Environ Sci* 10:914766. <https://doi.org/10.3389/fenvs.2022.914766>
- Keiluweit M, Bougoure JJ, Nico PS, Pett-Ridge J, Weber PK, Kleber M (2015) Mineral protection of soil carbon counteracted by root exudates. *Nat Clim Change* 5:588–595. <https://doi.org/10.1038/nclimate2580>
- Kiani M, Raave H, Simojoki A, Tammeorg O, Tammeorg P (2021) Recycling lake sediment to agriculture: effects on plant growth, nutrient availability, and leaching. *Sci Total Environ* 753:141984. <https://doi.org/10.1016/j.scitotenv.2020.141984>
- Kopittke PM, Berhe AA, Carrillo Y, Cavagnaro TR, Chen D, Chen Q-L, Román Dobarco M, Dijkstra FA, Field DJ, Grundy MJ, He J-Z, Hoyle FC, Kögel-Knabner I, Lam SK, Marschner P, Martinez C, McBratney AB, McDonald-Madden E, Menzies NW, Mosley LM, Mueller CW, Murphy DV, Nielsen UN, O'Donnell AG, Pendall E, Pett-Ridge J, Rumpel C, Young IM, Minasny B (2022) Ensuring planetary survival: the centrality of organic carbon in balancing the multifunctional nature of soils. *Crit Rev Environ Sci Technol* 52:4308–4324. <https://doi.org/10.1080/10643389.2021.2024484>
- Kuzyakov Y (2002) Factors affecting rhizosphere priming effects. *J Plant Nutr Soil Sci* 165:382–396. [https://doi.org/10.1002/1522-2624\(200208\)165:4%3c382::AID-JPLN382%3e3.0.CO;2-%23](https://doi.org/10.1002/1522-2624(200208)165:4%3c382::AID-JPLN382%3e3.0.CO;2-%23)
- Lehmann J (2007) Bio-energy in the black. *Front Ecol Environ* 5:381–387. [https://doi.org/10.1890/1540-9295\(2007\)5\[381:BITB\]2.0.CO;2](https://doi.org/10.1890/1540-9295(2007)5[381:BITB]2.0.CO;2)
- Lehmann J, Kleber M (2015) The contentious nature of soil organic matter. *Nature* 528:60–68. <https://doi.org/10.1038/nature16069>
- Lehmann J, Rillig MC, Thies J, Masiello CA, Hockaday WC, Crowley D (2011) Biochar effects on soil biota—a review. *Soil Biol Biochem* 43(9):1812–1836. <https://doi.org/10.1016/j.soilbio.2011.04.022>
- Lehmann J, Cowie A, Masiello CA, Kammann C, Woolf D, Amonette JE, Cayuela ML, Camps-Arbestain M, Whitman T (2021) Biochar in climate change mitigation. *Nat Geosci* 14:883–892. <https://doi.org/10.1038/s41561-021-00852-8>
- Liang C, Schimel JP, Jastrow JD (2017) The importance of anabolism in microbial control over soil carbon storage. *Nat Microbiol* 2:17105. <https://doi.org/10.1038/nmicrobiol.2017.105>
- Liu Z, Wu X, Liu W, Bian R, Ge T, Zhang W, Zheng J, Drosos M, Liu X, Zhang X, Cheng K, Li L, Pan G (2020) Greater microbial carbon use efficiency and carbon sequestration in soils: amendment of biochar versus crop straws. *GCB Bioenergy* 12:1092–1103. <https://doi.org/10.1111/gcbb.12763>
- Luo Y, Durenkamp M, De Nobili M, Lin Q, Devonshire BJ, Brookes PC (2013) Microbial biomass growth, following incorporation of biochars produced at 350 °C or 700 °C, in a silty-clay loam soil of high and low pH. *Soil Biol Biochem* 57:513–523. <https://doi.org/10.1016/j.soilbio.2012.10.033>
- Maestrini B, Nannipieri P, Abiven S (2015) A meta-analysis on pyrogenic organic matter induced priming effect. *GCB Bioenergy* 7:577–590. <https://doi.org/10.1111/gcbb.12194>
- Manzoni S, Taylor P, Richter A, Porporato A, Ågren GI (2012) Environmental and stoichiometric controls on microbial carbon-use efficiency in soils. *New Phytol* 196:79–91. <https://doi.org/10.1111/j.1469-8137.2012.04225.x>
- Manzoni S, Čapek P, Porada P, Thurner M, Winterdahl M, Beer C, Brüchert V, Frouz J, Herrmann AM, Lindahl BD, Lyon SW, Šantrůčková H, Vico G, Way D (2018) Reviews and syntheses: Carbon use efficiency from organisms to ecosystems—definitions, theories, and empirical evidence. *Biogeochemistry* 15:5929–5949. <https://doi.org/10.5194/bg-15-5929-2018>
- Melas GB, Ortiz O, Alacañiz JM (2017) Can biochar protect labile organic matter against mineralization in soil? *Pedosphere* 27:822–831. [https://doi.org/10.1016/S1002-0160\(17\)60421-1](https://doi.org/10.1016/S1002-0160(17)60421-1)
- Mganga KZ, Sietiö O-M, Meyer N, Poeplau C, Adamczyk S, Biasi C, Kalu S, Räsänen M, Ambus P, Fritze H, Pellikka PKE, Karhu K (2022) Microbial carbon use efficiency along an altitudinal gradient. *Soil Biol Biochem* 173:108799. <https://doi.org/10.1016/j.soilbio.2022.108799>
- Minasny B, Malone BP, McBratney AB, Angers DA, Arrouays D, Chambers A, Chaplot V, Chen ZS, Cheng K, Das BS, Field DJ, Gimona A, Hedley CB, Hong SY, Mandal B, Marchant BP, Martin M, McConkey BG, Mulder VL, O'Rourke S, Richer-de-Forges AC, Odeh I, Padarian J, Paustian K, Pan G, Poggio L, Savin I, Stolbovoy V, Stockmann U, Sulaeman Y, Tsui C-C, Vågten T-G, van Wesemael B, Winowiecki L (2017) Soil carbon 4 per mille. *Geoderma* 292:59–86. <https://doi.org/10.1016/j.geoderma.2017.01.002>
- Pan SY, Dong CD, Su JF, Wang PY, Chen CW, Chang JS, Kim H, Huang CP, Hung CM (2021) The role of biochar in regulating the carbon, phosphorus, and nitrogen cycles exemplified by soil systems. *Sustainability* 13(10):5612. <https://doi.org/10.3390/su13105612>

- Pei J, Li J, Mia S, Singh B, Wu J, Dijkstra FA (2021) Biochar aging increased microbial carbon use efficiency but decreased biomass turnover time. *Geoderma* 382:114710. <https://doi.org/10.1016/j.geoderma.2020.114710>
- Pietikäinen J, Kiikkilä O, Fritze H (2000) Charcoal as a habitat for microbes and its effect on the microbial community of the underlying humus. *Oikos* 89(2):231–242
- R Core Team (2022) A language and environment for statistical computing. R Foundation for Statistical Computing, Vienna, Austria
- Singh BP, Cowie AL (2014) Long-term influence of biochar on native organic carbon mineralisation in a low-carbon clayey soil. *Sci Rep* 4:3687. <https://doi.org/10.1038/srep03687>
- Sinsabaugh RL, Manzoni S, Moorhead DL, Richter A (2013) Carbon use efficiency of microbial communities: stoichiometry, methodology and modelling. *Ecol Lett* 16:930–939. <https://doi.org/10.1111/ele.12113>
- Soinne H, Hovi J, Tammeorg P, Turtola E (2014) Effect of biochar on phosphorus sorption and clay soil aggregate stability. *Geoderma* 219–220:162–167. <https://doi.org/10.1016/j.geoderma.2013.12.022>
- Tao F, Huang Y, Hungate BA, Manzoni S, Frey SD, Schmidt MWI, Reichstein M, Carvalhais N, Ciais P, Jiang L, Lehmann J, Wang Y-P, Houlton BZ, Ahrens B, Mishra U, Hugelius G, Hocking TD, Lu X, Shi Z, Viatkin K, Vargas R, Yigini Y, Omuto C, Malik AA, Guillermo P, Cuevas-Corona R, Di Paolo LE, Luotto I, Liao C, Liang Y-S, Saynes VS, Huang X, Luo Y (2023) Microbial carbon use efficiency promotes global soil carbon storage. *Nature* 618:981–985. <https://doi.org/10.1038/s41586-023-06042-3>
- Vance ED, Brookes PC, Jenkinson DS (1987) Microbial biomass measurements in forest soils: the use of the chloroform fumigation-incubation method in strongly acid soils. *Soil Biol Biochem* 19:697–702. [https://doi.org/10.1016/0038-0717\(87\)90051-4](https://doi.org/10.1016/0038-0717(87)90051-4)
- Wang J, Xiong Z, Kuzyakov Y (2016) Biochar stability in soil: meta-analysis of decomposition and priming effects. *GCB Bioenergy* 8:512–523. <https://doi.org/10.1111/gcbb.12266>
- Weng Z, Van Zwieten L, Singh BP, Kimber S, Morris S, Cowie A, Macdonald LM (2015) Plant-biochar interactions drive the negative priming of soil organic carbon in an annual ryegrass field system. *Soil Biol Biochem* 90:111–121. <https://doi.org/10.1016/j.soilbio.2015.08.005>
- Weng Z, Van Zwieten L, Singh BP, Tavakkoli E, Joseph S, Macdonald LM, Rose TJ, Rose MT, Kimber SWL, Morris S, Cozzolino D, Araujo JR, Archanjo BS, Cowie A (2017) Biochar built soil carbon over a decade by stabilizing rhizodeposits. *Nat Clim Change* 7:371–376. <https://doi.org/10.1038/nclimate3276>
- Weng Z, Van Zwieten L, Tavakkoli E, Rose MT, Singh BP, Joseph S, Macdonald LM, Kimber S, Morris S, Rose TJ, Archanjo BS, Tang C, Franks AE, Diao H, Schweizer S, Tobin MJ, Klein AR, Vongsivut J, Chang SLY, Kopittke PM, Cowie A (2022) Microspectroscopic visualization of how biochar lifts the soil organic carbon ceiling. *Nat Comm* 13:5177. <https://doi.org/10.1038/s41467-022-32819-7>
- Whitman T, Enders A, Lehmann J (2014) Pyrogenic carbon additions to soil counteract positive priming of soil carbon mineralization by plants. *Soil Biol Biochem* 73:33–41. <https://doi.org/10.1016/j.soilbio.2014.02.009>
- Woolf D, Amonette JE, Street-Perrott FA, Lehmann J, Joseph S (2010) Sustainable biochar to mitigate global climate change. *Nat Commun* 1:56. <https://doi.org/10.1038/ncomms1053>
- Woolf D, Lehmann J, Lee DR (2016) Optimal bioenergy power generation for climate change mitigation with or without carbon sequestration. *Nat Commun* 7:13160. <https://doi.org/10.1038/ncomms13160>
- Yan S, Yin L, Dijkstra FA, Wang P, Cheng W (2023) Priming effect on soil carbon decomposition by root exudate surrogates: a meta-analysis. *Soil Biol Biochem* 178:108955. <https://doi.org/10.1016/j.soilbio.2023.108955>
- Zhang Y, Sun C, Wang S, Xie H, Jiang N, Chen Z, Wei K, Bao X, Song X, Bai Z (2022) Stover and biochar can improve soil microbial necromass carbon, and enzymatic transformation at the genetic level. *GC Bioenergy* 14(10):1082–1096. <https://doi.org/10.1111/gcbb.12984>
- Zhang A, Wang X, Fang Y, Sun X, Tavakkoli E, Li Y, Wu D, Du Z (2023) Biochar more than stubble management affected carbon allocation and persistence in soil matrix: a 9-year temperate cropland trial. *J Soil Sediment* 23:3018–3028. <https://doi.org/10.1007/s11368-023-03546-3>
- Zhou S, Lin J, Wang P, Zhu P, Zhu B (2022) Resistant soil organic carbon is more vulnerable to priming by root exudate fractions than relatively active soil organic carbon. *Plant Soil*. <https://doi.org/10.1007/s11104-021-05288-y>
- Zimmerman AR, Gao B, Ahn M-Y (2011) Positive and negative carbon mineralization priming effects among a variety of biochar-amended soils. *Soil Biol Biochem* 43:1169–1179. <https://doi.org/10.1016/j.soilbio.2011.02.005>